ARTICLE

Modeling of Large-Scale Hydrogen Storage System Considering Capacity Attenuation and Analysis of Its Efficiency Characteristics

Junhui Li[1], Haotian Zhang[1], Cuiping Li[1,*], Xingxu Zhu[1], Ruitong Liu[2], Fangwei Duan[2] and Yongming Peng[3]

[1]Key Laboratory of Modern Power System Simulation and Control & Renewable Energy Technology,
Ministry of Education (Northeast Electric Power University), Jilin, 132012, China

[2]Ministry of Science and Technology, Electric Power Research Institute of State Grid Liaoning Electric Power Co., Ltd.,
Shenyang, 110006, China

[3]Northeast Electric Power Dispatching Control Center, Northeast Branch of State Grid Corporation of China,
Shenyang, 110180, China

*Corresponding Author: Cuiping Li. Email: licuipingabc@163.com

ABSTRACT

In the existing power system with a large-scale hydrogen storage system, there are problems such as low efficiency of electric-hydrogen-electricity conversion and single modeling of the hydrogen storage system. In order to improve the hydrogen utilization rate of hydrogen storage system in the process of participating in the power grid operation, and speed up the process of electric-hydrogen-electricity conversion. This article provides a detailed introduction to the mathematical and electrical models of various components of the hydrogen storage unit, and also establishes a charging and discharging efficiency model that considers the temperature and internal gas partial pressure of the hydrogen storage unit. These models are of great significance for studying and optimizing gas storage technology. Through these models, the performance of gas storage units can be better understood and improved. These studies are very helpful for improving energy storage efficiency and sustainable development. The factors affecting the charge-discharge efficiency of hydrogen storage units are analyzed. By integrating the models of each unit and considering the capacity degradation of the hydrogen storage system, we can construct an efficiency model for a large hydrogen storage system and power conversion system. In addition, the simulation models of the hydrogen production system and hydrogen consumption system were established in MATLAB/Simulink. The accuracy and effectiveness of the simulation model were proved by comparing the output voltage variation curve of the simulation with the polarization curve of the typical hydrogen production system and hydrogen consumption system. The results show that the charge-discharge efficiency of the hydrogen storage unit increases with the increase of operating temperature, and H_2 and O_2 partial voltage have little influence on the charge-discharge efficiency. In the process of power conversion system converter rectification operation, its efficiency decreases with the increase of temperature, while in the process of inverter operation, power conversion system efficiency increases with the increase of temperature. Combined with the efficiency of each hydrogen storage unit and power conversion system converter, the upper limit of the capacity loss of different hydrogen storage units was set. The optimal charge-discharge efficiency of the hydrogen storage system was obtained by using the Cplex solver at 36.46% and 66.34%.

KEYWORDS

Hydrogen storage system; simulation modeling; electrolyzer; fuel cell; capacity loss

1 Introduction

The Guiding Opinions on Accelerating the Development of New Energy Storage issued by the National Development and Reform Commission and the National Energy Administration in July 2021 [1], stating that hydrogen energy is regarded as "new energy storage", which indicates that hydrogen energy storage has great development prospects. Compared with other electrochemical energy storage, hydrogen energy storage is a green energy storage technology, which can be used in scenarios such as absorbing renewable energy, grid peak shaving and valley filling, and microgrid. However, there are few studies on the charge-discharge efficiency, hydrogen production and hydrogen consumption flow rates of hydrogen storage systems. In order to better understand the performance of hydrogen storage systems (HSS) and provide a basis for their participation in power system peak shaving and capacity allocation [2], it is necessary to conduct in-depth research and analysis of the internal characteristics of the entire hydrogen storage system.

The electrochemical reaction of the HSS during charging and discharging is a nonlinear process affected by many factors. In terms of electrical engineering applications, in order to facilitate research, common electrical components are used, and the external characteristics of the voltage and current of the hydrogen storage system during the charging and discharging process are connected, and an equivalent circuit model is constructed to clearly describe the charging and discharging characteristics of the HSS. In terms of battery characteristics analysis and modeling, Li et al. [3] constructed a third-order dynamic model of lead-acid batteries, which provided a basis for the rational use of lead-acid batteries and state monitoring; He et al. [4] introduced three modeling methods for the operating efficiency and life decay of electrochemical energy storage systems; Feng et al. [5] comprehensively considered factors such as battery capacity, temperature, and rate, and analyzed the power battery terminal voltage and ohmic polarization, electrical The relationship between chemical polarization, concentration polarization, unbalanced potential, hysteresis characteristics and other factors, a dynamic comprehensive equivalent circuit model is proposed to analyze the battery characteristics; Li et al. [6] based on the working mechanism and external characteristics of vanadium redox batteries, we have established a battery simulation model. Through this model, we studied the voltage and current loss characteristics of vanadium redox batteries under rated power charging and discharging modes, and measured the changes in charging and discharging efficiency at low temperatures under different power levels; Liu [7] analyzed a charging and discharging efficiency model for lithium iron phosphate batteries was established and the factors affecting efficiency were analyzed.

For the research on the characteristics of each part of the hydrogen storage system, Liu et al. [8] introduced the characteristics of hydrogen energy storage and the current mathematical model of electricity-hydrogen energy storage; Qin et al. [9] established a wind-hydrogen coupled system model, and has Modeling of hydrogen storage and hydrogen consumption; Ren et al. [10] considered the physical characteristics of the HSS, and established a high-pressure hydrogen storage tank operation model based on Fan's equation; Gu et al. [11] detailed description of the various characteristics of proton exchange membrane fuel cells and construction of its simulation model; Farrukh et al. [12] established mathematical models of electrolytic cells and fuel cells, and studied the effects of various parameters on system energy efficiency and external energy efficiency from an energy perspective. At the same time, we also considered the participation of hydrogen storage systems; Cai et al. [13] mainly focused on the hydrogen consumption and durability characteristics of fuel cells, and proposes an optimal control method for multi series fuel cell systems that considers system hydrogen consumption and durability, in order to reduce system hydrogen consumption and extend service life; Cai et al. [14] combined the electrochemical characteristics, gas flow, and temperature of proton exchange membrane fuel cells, taking into account the efficiency and lifespan of fuel cells, and establishes a customized dynamic

power generation system model based on PSCAD/EMTDC, and a grid-connected control strategy is proposed; Cai et al. [15] analyzed the power exchange characteristics of heterogeneous energy sources in the wind/solar hydrogen production system, establishes a homogenization analysis model of the wind/solar hydrogen production system, analyzes the operating point law and the operating point index range, analyzes the system operation domain and makes a reasonable analysis.

For the existing research on hydrogen storage system, Amir et al. [16] analyzed an innovative combination of solar cells has been established based on parabolic trough collectors and proton exchange membrane electrolyzers and fuel cell as a new green hydrogen production configuration from the perspective of thermodynamics and actual economy; Seyed et al. [17] proposed A new hybrid energy production/storage system has been proposed, including compressed air energy storage, a Brayton cycle driven by a heliostat, and a hydrogen production device. This system can reduce the pollutant emissions of compressed air energy storage technology, and has the advantages of high efficiency and environmental protection; Rama et al. [18] mainly introduced the importance of existing porous materials, polymers, metals and composite metal hydrides in solid hydrogen storage, and emphasized the importance of catalysts; a new hydrogen production system has been constructed using medical waste and zero carbon emissions biogas [19]. The system consists of plasma gasification, solid oxide fuel cells, steam turbine cycles, and autothermal reforming. This system can efficiently utilize waste resources and achieve a zero carbon emission hydrogen production process; research has been conducted on comprehensive efficiency [20], hydrogen production rate, and economic efficiency, and the use of cement waste heat through the Rankine cycle to generate the required electrical energy for the operation of PEM electrolytic cells; the power allocation degradation problem in multi stack fuel cell systems was considered to meet the load power requirements [21].

Research on System Capacity Decay Characteristics, Liu et al. [22] used FLUENT software to establish a numerical model for the leakage and diffusion of high-pressure hydrogen storage tanks, and studied its influencing factors. This method can be used to simulate the leakage and diffusion process of high-pressure hydrogen storage tanks, which helps to evaluate and optimize relevant safety measures. Li et al. [23] tested the durability of fuel cells through power generation-electrolysis cycle experiments, and analyzed the reasons for fuel cell performance degradation through electrochemical impedance spectroscopy and microphysical characterization methods. Zhu et al. [24] has been established to describe the aging degree of metal hydrogen storage tanks, based on the pressure composition temperature curve of the hydrogenation process of metal hydrogen storage tanks. This model can be used to evaluate the aging of hydrogen storage tanks and provide a reference for the maintenance and replacement of hydrogen storage tanks. Xu et al. [25] took 18650 NCM811 lithium-ion battery as the research object to study the influencing factors of the capacity decay of lithium-ion battery. Zhao et al. [26] conducted node tests on lithium titanate batteries for a specific number of cycles, and used the Arrhenius formula to establish a capacity decay characteristic curve.

Current research may not fully consider the factors of the entire hydrogen storage system when modeling hydrogen storage systems, and there are few literature describing the relationship between temperature and pressure on the charging and discharging efficiency of hydrogen storage systems. In addition, there is a lack of detailed description of the factors that affect the capacity decay characteristics of hydrogen storage systems. Therefore, future research can continue to explore the modeling of the entire hydrogen storage system, and delve into the effects of temperature and pressure on the charging and discharging efficiency of the hydrogen storage system, while analyzing and describing the factors that affect the capacity attenuation characteristics of the hydrogen storage system.

In this paper, the capacity attenuation characteristic equation applicable to the hydrogen storage system is constructed first considering the system capacity attenuation. On this basis, the simulation models of each part and the whole of the large-scale hydrogen storage system are established, and the mathematical models and electrical models of each unit of the hydrogen storage system are introduced. The physical meaning of each part is analyzed. The hydrogen storage system is systematically simulated and analyzed in MATLAB/Simulink using the electrical model. The validity of the simulation model is proved by comparing the polarization curves of typical hydrogen production and hydrogen consumption systems. Finally, the optimal charging and discharging efficiency of hydrogen storage system considering the capacity attenuation factor is obtained by synthesizing the unit model.

2 Network Structure of Large-Scale Hydrogen Storage System

The simplified structure of the power system with hydrogen storage system is shown in Fig. 1. The DC bus connects the large-scale hydrogen storage system with the public power grid and the photovoltaic power generation system. The large-scale hydrogen storage system constructed in this paper refers to a large-scale system consisting of a collection of multiple internal hydrogen storage units and an external power conversion system (PCS) converter. Each hydrogen storage unit includes a hydrogen production unit (PEM electrolyzer), a hydrogen storage tank and a hydrogen consumption unit (Proton exchange membrane fuel cell) [27]. Each electrolyzer unit and fuel cell unit are connected in series and parallel. Hydrogen production needs to meet the needs of local industries. By connecting the photovoltaic system, cheap renewable energy can be used to power the electrolyzer to obtain hydrogen and oxygen, which can be stored in the hydrogen storage tank. Acceptable electrical energy is delivered to the grid and can also reduce the amount of electricity purchased from the grid [28]. Since the actual electricity-to-hydrogen-to-electricity conversion efficiency is not high, it is necessary to study the characteristics of each part of the hydrogen storage system more specifically to improve its energy conversion efficiency within the artificially controllable range [29]. Based on this, this paper combines the mathematical model and electrical model of each part of the hydrogen storage system for simulation.
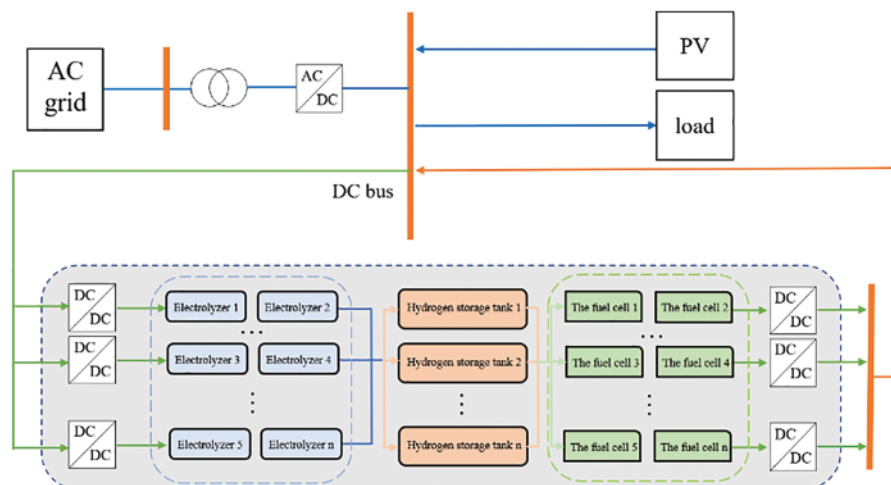

Figure 1: Structure of power system with hydrogen storage system

3 Simulation Model of Large-Scale Hydrogen Storage System

3.1 Simulation Model of Hydrogen Storage System

The hydrogen storage system consists of multiple electrolytic cell units, hydrogen storage tanks, and multiple fuel cell units. After the system is connected to the power grid, each electrolytic cell unit generates hydrogen gas and compresses it into a hydrogen storage tank. When electrical energy is needed, each fuel cell unit converts the hydrogen stored in the hydrogen storage tank into electrical energy.

Due to the different internal characteristics of each electrolyzer unit and fuel cell unit, and when the internal temperature and gas pressure of the hydrogen storage system are different, the charge and discharge efficiency will also change accordingly. Considering the series-parallel combination of the monomer model, the construction is composed of the large-scale hydrogen storage system is shown in Fig. 2.
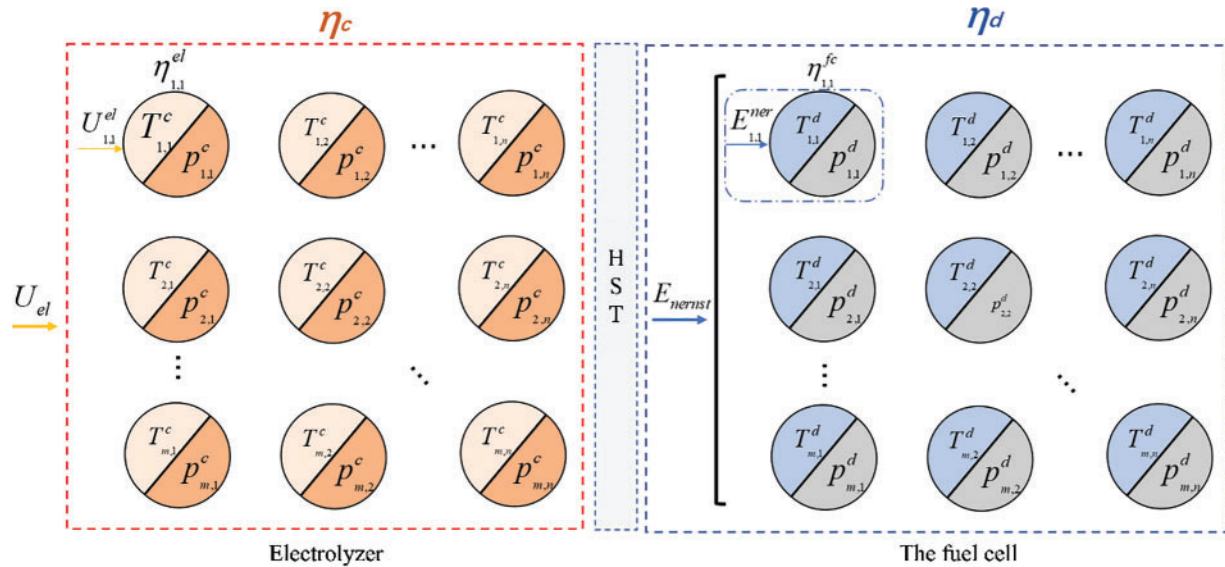

Figure 2: Simplified structure of large-scale hydrogen storage system

Assume that the temperature set and pressure set of each single cell in the series-parallel combination are $T_{i,j}^c = \left\{ T_{1,1}^c, \cdots, T_{m,n}^c \right\}$ and $p_{i,j}^c = \left\{ p_{1,1}^c, \cdots, p_{m,n}^c \right\}$. The corresponding cell input voltage and the efficiency of each cell are $U_{i,j}^{el} = \left\{ U_{1,1}^{el}, \cdots, U_{m,n}^{el} \right\}$ and $\eta_{i,j}^{el} = \left\{ \eta_{1,1}^{el}, \cdots, \eta_{m,n}^{el} \right\}$.

The temperature and pressure set for each single fuel cell are $T_{i,j}^d = \left\{ T_{1,1}^d, \cdots, T_{m,n}^d \right\}$ and $p_{i,j}^d = \left\{ p_{1,1}^d, \cdots, p_{m,n}^d \right\}$, the corresponding fuel cell thermodynamic electromotive force and fuel cell efficiency are $E_{i,j}^{ner} = \left\{ E_{1,1}^{ner}, \cdots, E_{m,n}^{ner} \right\}$ and $\eta_{i,j}^{fc} = \left\{ \eta_{1,1}^{fc}, \cdots, \eta_{m,n}^{fc} \right\}$.

m and n are the number of parallel and series connected large-scale hydrogen storage systems, respectively.

From this, the formulas for the charge and discharge efficiency of large-scale hydrogen storage systems are obtained as follows:

$$\eta_c = \sum_{i=1}^{m}\sum_{j=1}^{n} U_{i,j}^{el}\eta_{i,j}^{el} \Big/ \sum_{i=1}^{m}\sum_{j=1}^{n} U_{i,j}^{el} \tag{1}$$

$$\eta_d = \sum_{i=1}^{m}\sum_{j=1}^{n} E_{i,j}^{ner}\eta_{i,j}^{fc} \Big/ \sum_{i=1}^{m}\sum_{j=1}^{n} E_{i,j}^{ner} \tag{2}$$

where η_c and η_d are the charging and discharging efficiencies, respectively.

The energy conversion efficiency of PCS (Power Conversion System) in hydrogen storage systems during external charging and discharging processes will also have an impact on the efficiency of the entire large-scale hydrogen storage system. In addition to considering the impact of internal characteristics of large hydrogen storage systems on efficiency, it is also necessary to consider the impact of PCS energy conversion efficiency on the efficiency of the entire hydrogen storage system. The efficiency of PCS has a nonlinear relationship with the output power of the hydrogen storage system [30], The efficiency of PCS is as follows:

$$\eta_{pcs} = x\left(\frac{P_A}{P_N}\right) + y \tag{3}$$

where P_A/P_N is the per-unit value of the output power, and x, y are the piecewise linearization coefficients.

In summary, the total charge-discharge efficiency of the large-scale hydrogen storage system is:

$$\begin{aligned}\eta_{c,z} &= \eta_c\eta_{PCS}\\ \eta_{d,z} &= \eta_d\eta_{PCS}\end{aligned} \tag{4}$$

In the actual production process, the capacity of the hydrogen storage system will gradually decrease due to a decrease in the number of cycles. The changes in working temperature and internal pressure within the system will have an impact on the absorption and release of hydrogen in the hydrogen storage system, and thus affect the capacity of the hydrogen storage system. In order to better fit the engineering practice, The capacity decay effect formula [22–24] that affects the capacity decay of the hydrogen storage system is:

$$\begin{aligned}r_1 &= 3.714 \times cycle + 0.1651\\ r_2 &= -7.585 \times cycle + 360\\ r_3 &= 0.232 \times T - 8.927\\ r_4 &= -0.164 \times T + 14.26\end{aligned} \tag{5}$$

$$Q_{less} = 1 - \left(\frac{r_1}{282.74} + \frac{r_2}{(1 + \exp(r_3 \times p + r_4))\,282.74}\right) \tag{6}$$

where Q_{loss} is the capacity loss rate, r influence coefficient of reaction temperature and number of cycles on capacity loss, T is the working temperature, p is the working pressure. $cycle$ is the number of battery cycles.

According to the above formula, the total life loss of the hydrogen storage system is:

$$Q_{z\_loss} = \sum_{r=1}^{N} Q_{less,r}/N \tag{7}$$

where $Q_{less,r}$ is the capacity loss of hydrogen storage units, and N is the number of hydrogen storage units.

3.2 Hydrogen Storage Unit Model

3.2.1 Mathematical Model

1) Electrolyzer Model

The electrolytic cell voltage model is derived from the relationship between the electrolysis voltage and electrolytic current [31], and the single electrolytic cell voltage model can be expressed by the following formula:

$$U_{el} = E + U_{el,act} + U_{el,ohm} \tag{8}$$

where E is the open circuit voltage of the electrolytic cell, $U_{el,act}$ is the activation polarization overvoltage, and $U_{el,ohm}$ is the ohmic polarization overvoltage.

In an electrolytic cell, the open circuit voltage is related to temperature and the activity of each component involved in the reaction. The open circuit voltage of the electrolytic cell can be derived through the Nernst equation. This equation is used to calculate the equilibrium voltage of a specific redox pair on the electrode relative to the standard potential:

$$E = E_0 + \frac{RT_{el}}{zF} \ln\left(\frac{P_{H_2} P_{O_2}^{0.5}}{a_{H_2O}}\right) \tag{9}$$

where E_0 is the standard electromotive force, T_{el} is the cell temperature, a_{H_2O} is the water activity between the anode and the electrolyte, P_{H_2} is the partial pressure of hydrogen at the anode, and P_{O_2} is the partial pressure of oxygen at the cathode.

The standard electromotive force expression is:

$$E_0 = \Delta G / zF \tag{10}$$

where ΔG is the Gibbs free energy change of the electrochemical reaction process; z is the number of electrons transferred per reaction; F is the Faraday constant.

$$U_{el,act} = \left(s_1 + s_2 T_{el} + s_3 T_{el}^2\right) \ln\left(\frac{t_1 + t_2/T_{el} + t_3/T_{el}^2}{A_{el}} I_{el} + 1\right) \tag{11}$$

where T_{el} is the temperature of the electrolytic cell; A_{el} is the area of the electrolysis module; I_{el} is the DC current; s_n is the electrode overvoltage coefficient ($n = 1, 2, 3$), and t_p is the electrode overvoltage coefficient ($p = 1, 2, 3$).

The ohmic polarization overvoltage is:

$$U_{el,ohm} = \frac{r_1 + r_2 T_{el}}{A_{el}} I_{el} \tag{12}$$

where r_1 and r_2 are the ohmic resistance parameters of the electrolyte.

The cell efficiency formula is equal to the ratio of the input voltage inside the cell to the voltage at the cell port.

$$\eta_{el} = E / U_{el} \tag{13}$$

2) Fuel cell model

The output voltage of a single fuel cell [32] port can be expressed as:

$$U_{fc} = E_{nernst} - U_{fc,act} - U_{fc,ohm} - U_{fc,conc} \tag{14}$$

where E_{nernst} is the thermodynamic electromotive force; $U_{fc,act}$ is the activation overvoltage; $U_{fc,ohm}$ is the ohmic overvoltage; $U_{fc,conc}$ is the concentration overvoltage.

Thermodynamic electromotive force means that the work done to transfer electrons during the H_2 combustion reaction is equal to the Gibbs free energy released during the reaction without considering the loss, expressed by the Nernst equation and the Gibbs free energy change.

$$E_{nernst} = \frac{\Delta G}{2F} + \frac{\Delta S}{2F} (T_{fc} - T_{ref}) + \frac{RT_{fc}}{2F} \left[\ln (P_{H_2}) + \frac{1}{2} \ln (P_{O_2}) \right] \tag{15}$$

where ΔG is the Gibbs free energy change of the chemical reaction; F is the Faraday constant; ΔS is the change in entropy; T_{fc} is the fuel cell temperature; T_{ref} is the reference temperature; R is the gas constant; P_{O_2} is the partial pressure of hydrogen at the anode catalyst/gas interface.

The activation polarization overvoltage is mainly manifested as a slow rate phenomenon when the electrode surface is just about to activate the electrochemical reaction, which is generally expressed by a fixed parameter.

$$U_{act} = [\xi_1 + \xi_2 T_{fc} + \xi_3 T_{fc} \ln (C_{O2}) + \xi_4 \times T_{fc} \times \ln (I_{fc})] \tag{16}$$

$$C_{O2} = P_{O2}/5.08 \times 10^6 \exp (-498/T_{fc}) \tag{17}$$

where ζ_{1234} is the empirical parameter; I_{fc} is the current of the fuel cell module; C_{O2} is the oxygen concentration of the cathode gas and liquid surface; P_{O2} is the oxygen interface partial pressure of the fuel cell.

The ohmic overvoltage of the PEMFC module is mainly caused by the voltage drop generated by the membrane impedance corresponding to the proton membrane, which is equivalent to the voltage drop generated by the internal resistance of the fuel cell.

$$U_{ohm} = I_{fc} R_{obm} = I_{fc} (r_M l/A + R_c) \tag{18}$$

$$r_M = \frac{181.6 \left[1 + 0.03 \left(\frac{I_{fc}}{A} \right) + 0.062 \left(\frac{T_{fc}}{303} \right)^2 \left(\frac{I_{fc}}{A} \right)^{2.5} \right]}{\left[\lambda - 0.634 - 3 \left(\frac{I_{fc}}{A} \right) \right] \exp \left[4.18 \left(\frac{T_{fc} - 303}{T_{fc}} \right) \right]} \tag{19}$$

where l is the thickness of the membrane; r_M is the resistivity of the membrane; R_c is the resistance that prevents protons from passing through the membrane; A is the effective area of the membrane.

The concentration overvoltage of the PEMFC module mainly occurs in the working state of high current. At this time, the electrochemical reaction is too fast, which causes the slow diffusion of reactants or products and the restriction of mass transfer of reactants. The mathematical expression is as follows:

$$U_{conc} = -B \ln (1 - J/J_{max}) \tag{20}$$

where J and J_{max} are the current density and the maximum current density, respectively; B is the equation constant, which is determined by the battery operating conditions.

The current density is:

$$J = I_{fc}/A \tag{21}$$

The fuel cell efficiency formula is equal to the ratio of the output voltage of the fuel cell port to the thermodynamic electromotive force of the internal reaction.

$$\eta_{fc} = U_{fc}/E_{nernst} \tag{22}$$

3) Hydrogen storage tank model

The hydrogen production flow rate of a single electrolyzer is [33]:

$$V_{el,H_2} = \frac{I_{el}}{zF} = \frac{I_{el}E}{zFE} = \frac{P_{c,in}}{zFE} \tag{23}$$

The principle of hydrogen consumption molar flow rate is the same as above:

$$V_{fc-H_2} = \frac{I_{fc}}{zF} = \frac{I_{fc}E_{nernst}}{zFE_{nernst}} = \frac{P_{d,out}}{zFE_{nernst}} \tag{24}$$

Hydrogen storage:

$$M_{H_2} = \int_{t_1}^{t_2} \left(V_{el\_H_2} - V_{fc\_H_2} \right) \mathrm{d}t \tag{25}$$

3.2.2 Electrical Model

1) Equivalent circuit model of electrolyzer

The electrolytic cell model can be equivalent to the charging process, so the electrolytic cell can be considered as an equivalent power source. In an electrolytic cell, internal current flows from the positive pole of the power supply to the negative pole. However, the direction of overvoltage caused by activation polarization loss and ohmic overvoltage is opposite to the direction of open circuit voltage. That is to say, the effects of activated polarization and ohmic overvoltage will require a higher voltage than the open circuit voltage for the actual electrolysis process to proceed. Ohmic loss is mainly caused by the current passing through electrode materials, connecting components, liquid junction potential when in contact with different solutions, and the resistance of ions in the electrolyte. The relationship between Ohm voltage loss and current follows Ohm's law, which means that voltage loss is equal to current multiplied by resistance. Polarization loss is mainly caused by the deviation of cell equilibrium potential caused by changes in concentration in the electrolytic cell. When the electrolyte concentration changes, polarization loss can lead to a difference between the working voltage and open circuit voltage of the electrolytic cell. In summary, ohmic loss and polarization loss are the two main factors causing voltage loss in the electrolysis process.

According to the above analysis, the equivalent circuit model of the electrolytic cell [34] is shown in Fig. 3.

According to the equivalent circuit and mathematical model, a simulation model is built through MATLAB/Simulink [35], as shown in Fig. 4. Refer to Appendix A for each model parameter. In order to reflect the characteristics of the electrolytic cell model, the voltage and current constraints during charging and discharging are not considered for the time being.
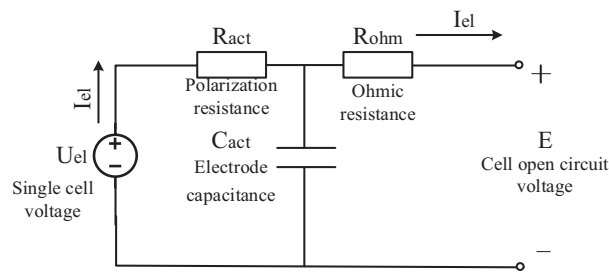
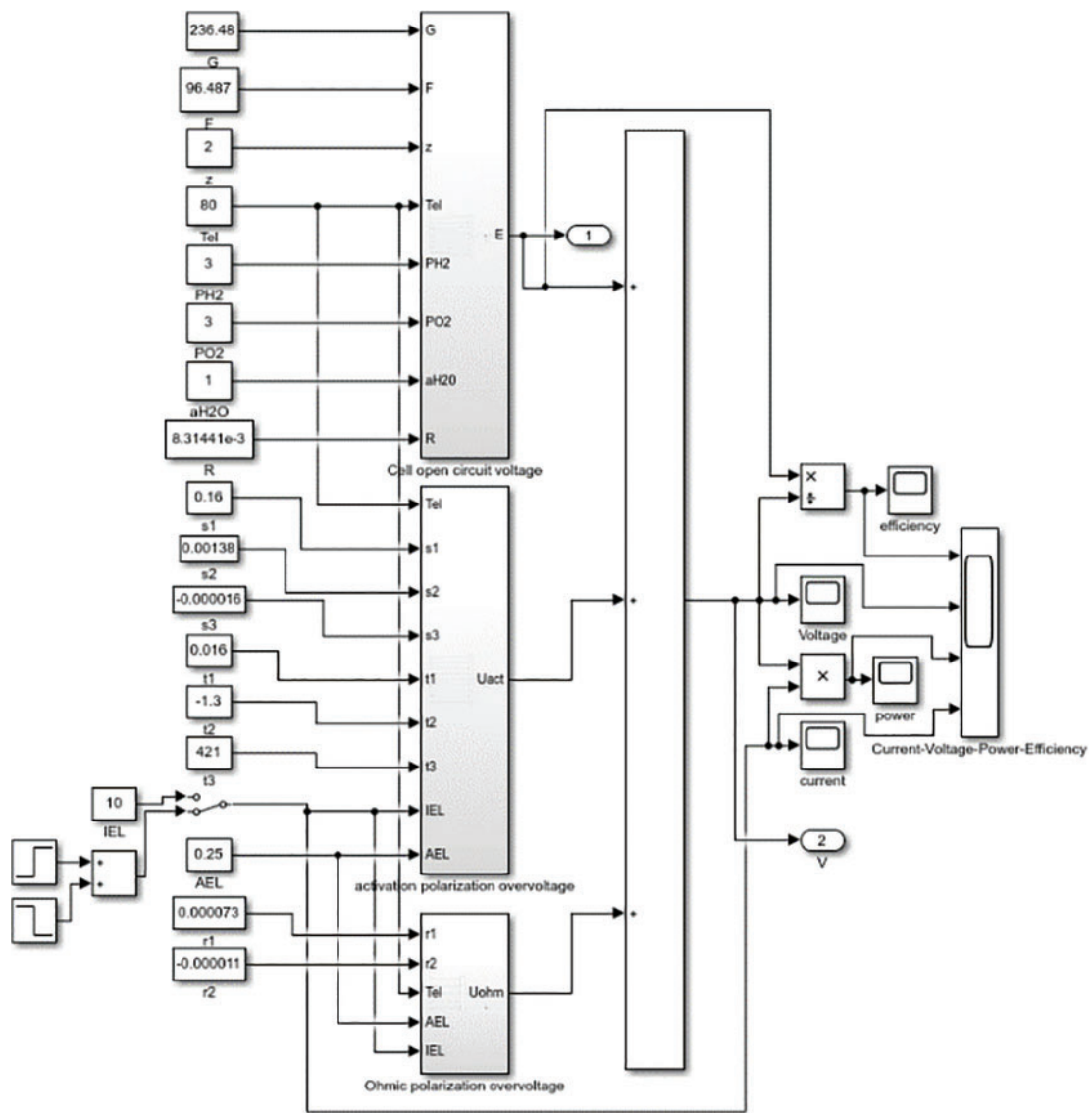**Figure 3:** Electrolyzer equivalent circuit model

Figure 4: Electrolyzer simulation model

2) Equivalent circuit model of fuel cell

Since a series of physical and chemical changes will occur on the positive and negative electrodes of the fuel cell during operation, each process will generate a certain resistance. In order to make the reaction on the electrodes continue to occur, it needs to consume its own energy to overcome the resistance. During this process, the electrode potential shift phenomenon will occur, and the losses generated during the reaction include activation polarization voltage, ohmic polarization voltage and concentration overvoltage. The corresponding fuel cell equivalent circuit model [36] is shown in Fig. 5.
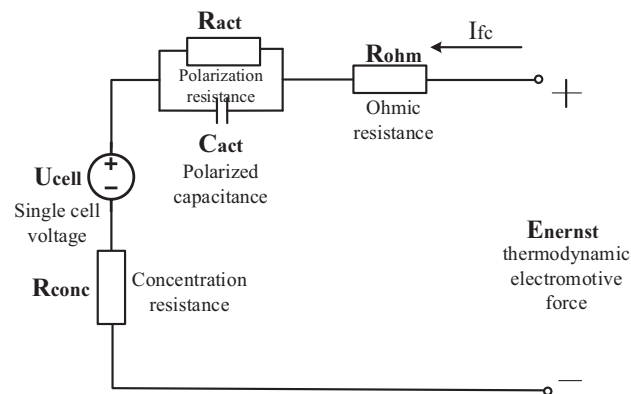

Figure 5: Equivalent circuit diagram of single fuel cell

The fuel cell simulation model structure [37] is shown in Fig. 6. The fuel cell reaction is equivalent to the discharge process in the entire hydrogen storage system, where the thermodynamic electromotive force is equivalent to the internal voltage of the fuel cell, and U_{fc} is equivalent to the output voltage of the fuel cell.

4 Example Analysis

In order to verify the validity of the model established in this paper, some parameters are set as shown in Appendix A [38]. Combined with the simulation model of the PEM electrolyzer and Proton exchange membrane fuel cell built in Simulink, the variation of the voltage of the electrolyzer and the fuel cell with the current is obtained. Figs. 7 and 8 respectively show the variation of the input voltage of the electrolyzer and the output voltage of the fuel cell with current and the typical polarization curves of the above-mentioned electrolyzer and fuel cell. It can be seen from the figure that the variation trend of the voltage and current of the electrolyzer and the fuel cell model constructed in this paper and the typical polarization curves of the two, which shows the correctness and effectiveness of the simulation model established in this paper.
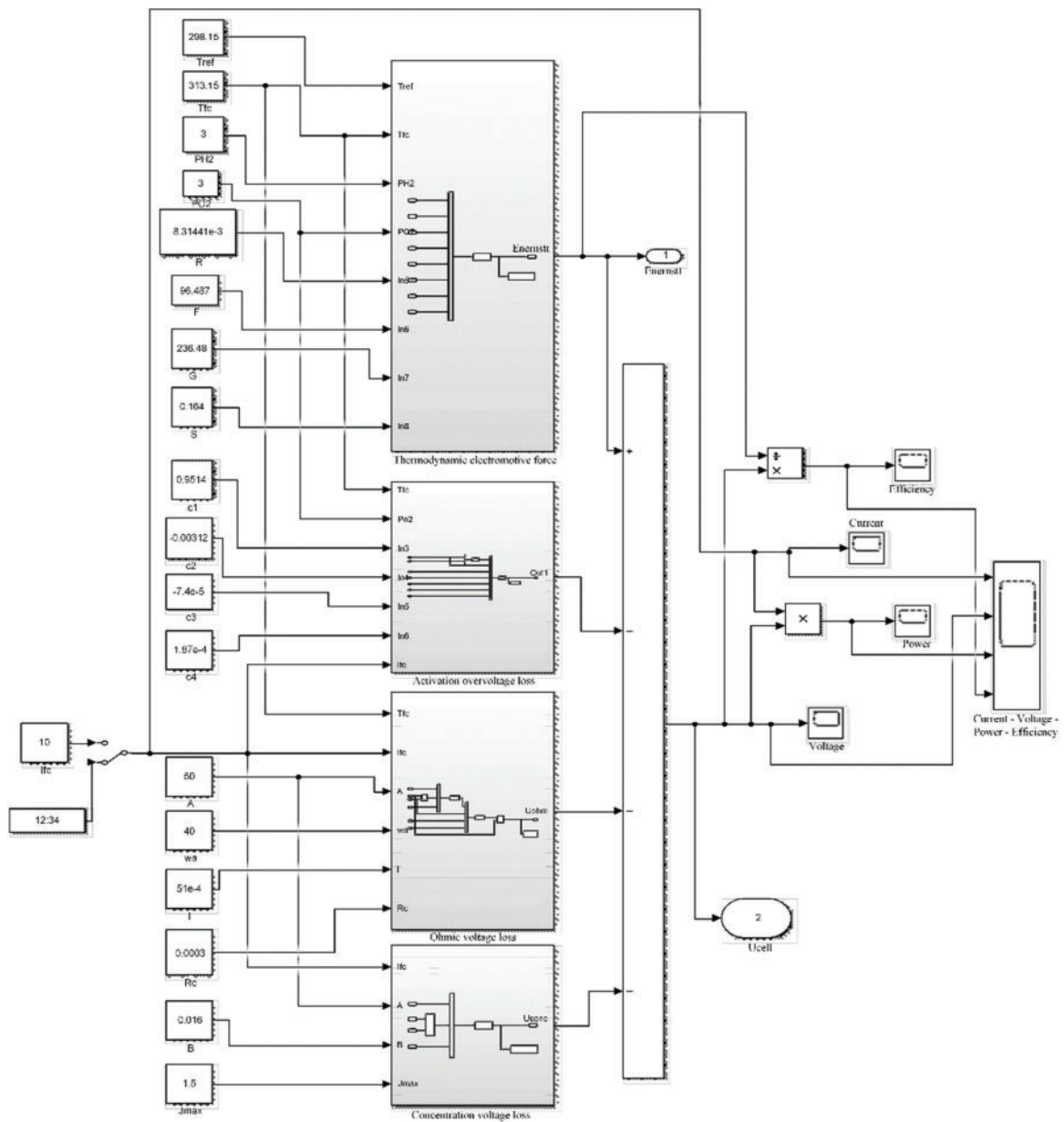
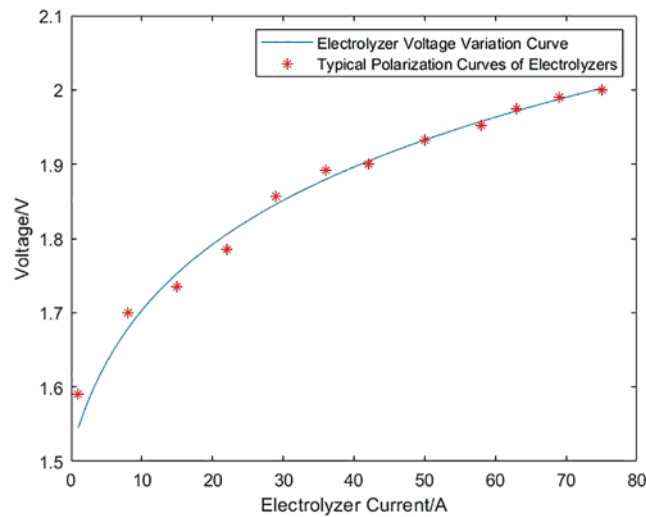**Figure 6:** Fuel cell simulation structure diagram

Figure 7: Comparison between the input voltage and current curve of the electrolyzer and the typical polarization curve
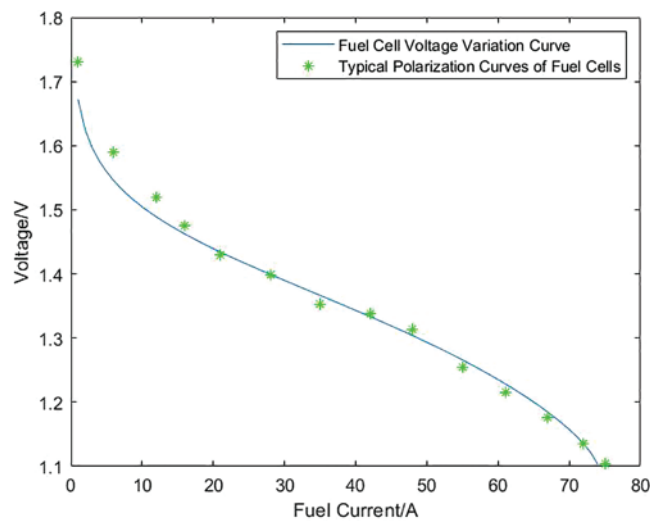

Figure 8: Comparison of output voltage *vs*. current curve of fuel cell and typical polarization curve

4.1 Analysis of the Influence of Hydrogen Storage Unit Efficiency

In order to analyze the influence of temperature and partial gas pressure of each part of the hydrogen storage unit on the charging and discharging efficiency of the hydrogen storage unit, the hydrogen storage unit is charged and discharged under the constant current of 10, 30, 50 and 70 A, that is, the current density is 0.04, 0.12, 0.2 and 0.28 A/cm². Figs. 9 and 10 show the variation curves of hydrogen storage unit charge-discharge efficiency with operating temperature and gas partial pressure under each constant current density charge-discharge state.
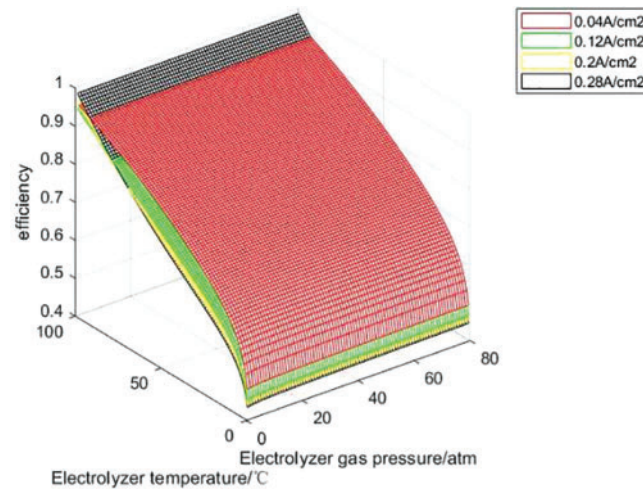
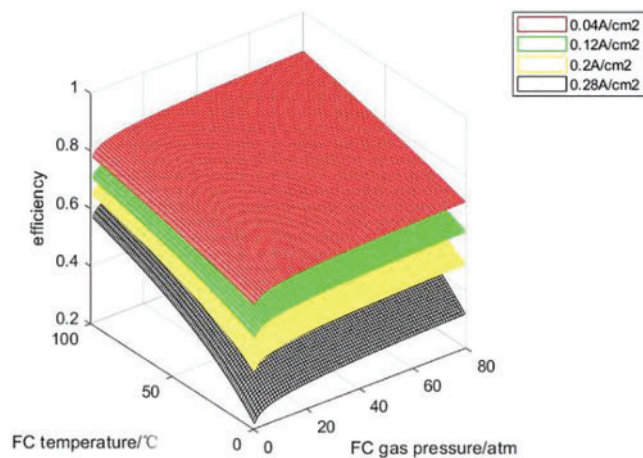**Figure 9:** Charge efficiency curves at constant current density

Figure 10: Discharge efficiency curves under constant current density

It can be seen from Figs. 9 and 10 that under the condition of constant current density and constant gas partial pressure, the charge discharge efficiency of the hydrogen storage system increases with the increase of operating temperature, because the increase of temperature enhances the activity of the catalyst. When the system operating temperature and gas partial pressure are constant, the charging efficiency decreases with the increase of current density, because the increase of current leads to the increase of activation polarization overvoltage and ohmic polarization overvoltage in the electrolytic cell reaction, which leads to the decrease of efficiency; The discharge efficiency decreases with the increase of current density because the increase of current leads to the increase of activation over-voltage, ohmic over-voltage and concentration over-voltage during the fuel cell reaction process, which reduces the efficiency. At constant operating temperature and current density, with the increase of H_2 and O_2 partial pressure, the charging and discharging efficiency of the hydrogen storage system will increase, but the range is not large. Because changing the gas partial pressure will only affect the open circuit voltage of the electrolytic cell and the thermodynamic electromotive force and activation overvoltage of the fuel cell, H_2 and O_2 partial pressure have little effect on the charging and discharging

efficiency. With the increase of current, the voltage loss of electrolytic cell and fuel cell will increase, thus reducing the charge discharge efficiency. Theoretically, within the upper and lower limits of the current temperature and gas partial pressure settings, the optimal charging and discharging efficiency of the hydrogen storage unit can be 98.5% and 86.16%, respectively.

The PCS converter efficiency is strongly related to the output power of the large-scale hydrogen storage system. When considering the influence of the internal characteristics of the hydrogen storage system on the system charge and discharge efficiency, changes in the internal temperature and pressure of the system will also affect the power and lead to changes in the PCS efficiency. Figs. 11 and 12 describe the influence curves of temperature and pressure on PCS efficiency in the rectification process and the inversion process, respectively.
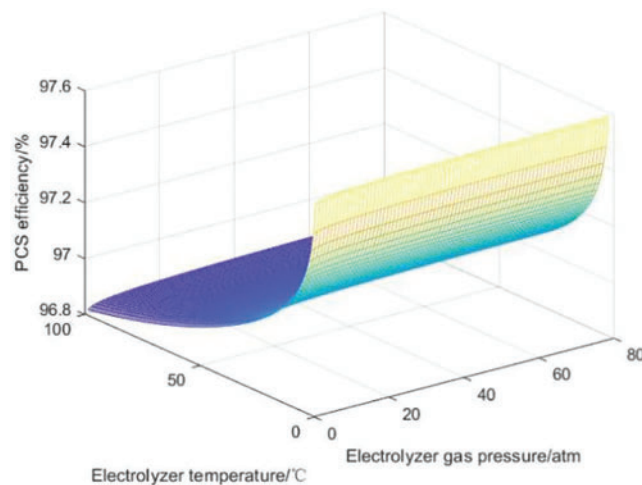

Figure 11: Influence curve of PCS efficiency in rectification process
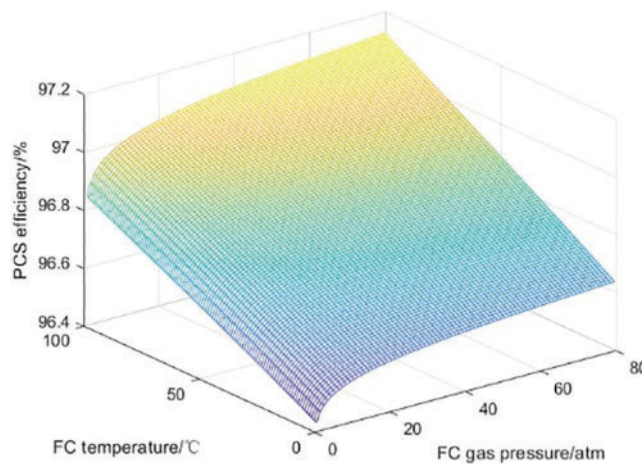

Figure 12: Inverting process PCS efficiency influence curve system

In the rectification stage of the PCS converter, as the temperature increases, the efficiency of the PCS converter will decrease, while the pressure has little effect on it. This is because during the rectification operation, power flows to the PCS converter, causing high current and low voltage,

resulting in poor heat dissipation conditions inside the converter. However, an increase in temperature will further reduce the heat dissipation effect, thus negatively affecting the rectification efficiency.

In the inverter operation of the PCS converter, the PCS efficiency increases with increasing temperature and slightly increases with increasing pressure. This is because during the operation of the inverter, power is output from the PCS, and at this time, the current is low and the voltage is high, making the requirements for heat dissipation relatively low. At the same time, a high-temperature environment is beneficial for improving the performance of certain components, thereby improving inverter efficiency. The reason why the impact of pressure on efficiency is relatively small may be due to the small impact of pressure changes on the working state of circuit components.

4.2 Analysis of the Influence of Hydrogen Storage Efficiency

In this paper, it is assumed that the capacity of the hydrogen storage tank is infinite, and the upper limit of the capacity decay rate is set to limit the quality of hydrogen that the hydrogen storage tank can hold. Since the partial pressure of the gas has little effect on the hydrogen storage unit, it is assumed that the partial pressure of the gas and the pressure in the tank are constant at 3 atm, the number of cycles of the hydrogen storage system is 2000 times, and the working environment is set to a constant temperature of 25°C. At this time, the capacity loss of the electrolyzer and the fuel cell increases with the increase of the internal working temperature, and the change curve of the capacity loss with temperature is shown in Fig. 13.
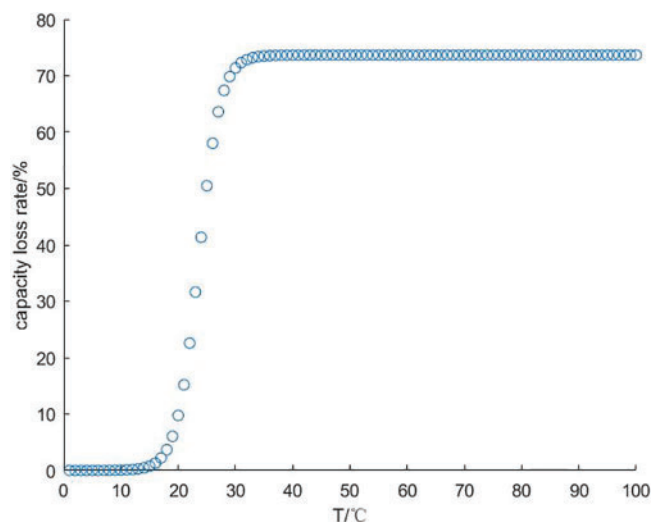

Figure 13: Capacity loss *vs*. temperature curve

Theoretically, if the temperature is kept at a high level, higher charge-discharge efficiency can be obtained, but in the actual production process, the capacity of the electrolyzer and fuel cell will decrease with the increase of temperature and the number of cycles. In order to be more practical, different upper limits of capacity decay are set for the hydrogen storage unit, as shown in Table 1, combined with the charge-discharge efficiency of the hydrogen storage unit and the influence curve of the PCS efficiency, and the Cplex solver is used to obtain the optimal value of the efficiency of the hydrogen storage system and the corresponding operating temperature.

Table 1: Hydrogen storage unit capacity decay upper limit

Electrolyzer unit number	Capacity loss upper limit/%	Fuel cell unit number	Capacity loss upper limit/%
1–10	70	1–10	30
11–20	60	11–20	40
21–30	50	21–30	50
31–40	40	31–40	60
41–50	30	41–50	70

It can be seen from Section 4.1 that the higher the working temperature of each unit electrolyzer and fuel cell, the higher the charge and discharge efficiency of the corresponding unit. Through calculation, it can be seen from Figs. 14 and 15 that after considering the capacity loss of the hydrogen storage unit, in the large-scale hydrogen storage system, each unit electrolyzer and fuel cell can no longer maintain the upper temperature limit. Through the solution, it is concluded that the optimal charging efficiency of the internal system of the hydrogen storage system is 63.46%, the PCS efficiency of the charging process is 97.57%, and the total charging efficiency of the system is 61.92%. The capacity loss of each unit is maintained within a controllable range, and the total system loss is 50%; The temperature range of a single fuel cell unit is between 22.9°C and 29.1°C, and it decreases with the decrease of the upper limit of capacity loss. Correspondingly, the optimal internal discharge efficiency of the hydrogen storage system is 68.34%, and the PCS efficiency during the discharge process is 97.09%. The total discharge efficiency of the system is 66.34%, and the total system capacity loss is 49.9%.
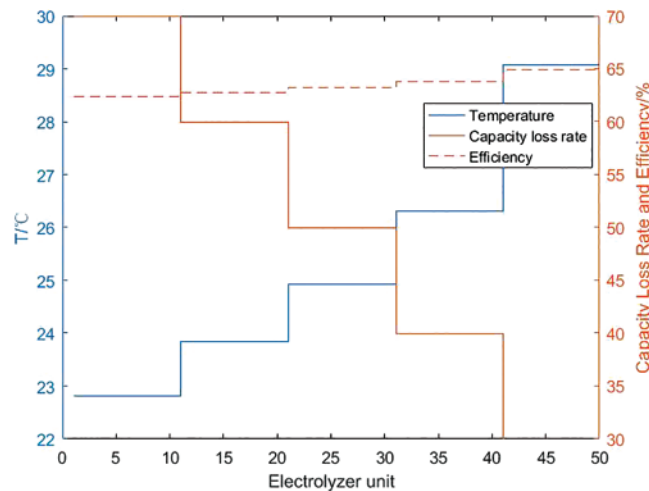

Figure 14: Calculation result of charging efficiency of hydrogen storage system
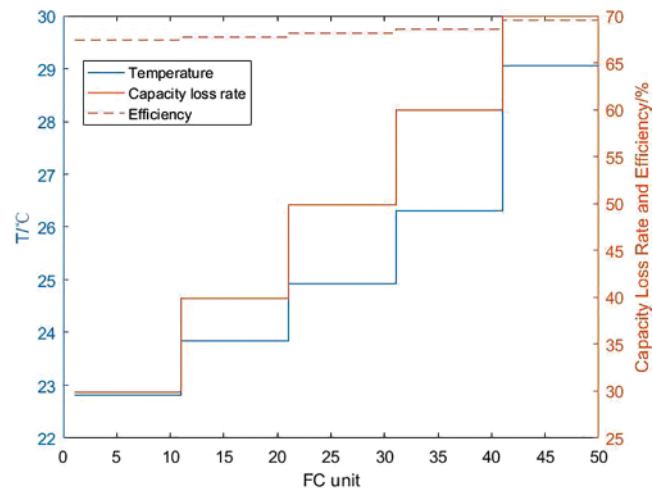
Figure 15: Calculation result of discharge efficiency of hydrogen storage system

5 Conclusion

In this paper, firstly, the attenuation characteristics of the battery are considered, and the simulation model of each part of the large-scale hydrogen storage system is systematically constructed in detail. Secondly, the steady-state simulation model of each component of the hydrogen storage unit is constructed, as well as the charge-discharge efficiency model and PCS efficiency model considering the temperature of the hydrogen storage system and the internal gas partial pressure. Through the simulation and modeling of the hydrogen storage system in MATLAB/Simulink, the efficiency characteristics of the hydrogen storage system and hydrogen storage unit are analyzed. With the goal of optimizing the efficiency of the large-scale hydrogen storage system, the results obtained by using the Cplex solver are as follows:

(1) The overall efficiency of a large-scale hydrogen storage system is affected by the internal characteristics of each hydrogen storage unit that makes up the system, including charging and discharging current, operating temperature, gas partial pressure and hydrogen storage tank capacity attenuation, as well as the efficiency of the PCS converter during AC/DC conversion with the outside world.

(2) Properly increasing the internal working temperature of the hydrogen storage unit can improve the charging and discharging efficiency of the system and the PCS efficiency during inverter operation, but will reduce the PCS efficiency during rectifier operation; Increasing H_2 and O_2 partial pressure can increase the efficiency of the hydrogen storage unit and PCS, but the increase is small, indicating that the pressure has little effect on the efficiency of the hydrogen storage system. The efficiency of the hydrogen storage unit will increase with the increase of charge-discharge current.

(3) The overall efficiency of the large-scale hydrogen storage system is linear with the system loss and working temperature. The capacity decay rate of the hydrogen storage tank increases with the temperature and changes fastest between 20°C and 30°C. Although the high working temperature will affect the capacity attenuation of the system, it will increase the charging and discharging efficiency. Under the above conditions, the optimal total charging efficiency of the system is 63.46%, and the total discharge efficiency is 66.34%.

To sum up the actual situation, in order to obtain appropriate charging and discharging efficiency and ensure that the system capacity loss is within a certain range, it is necessary to reasonably design the parameters.

Author Contributions: The authors confirm their contribution to the paper as follows: study conception: Junhui Li; design, data collection: Haotian Zhang; analysis and interpretation of results: Cuiping Li and Xingxu Zhu; draft manuscript preparation: Ruitong Liu, Fangwei Duan and Yongming Peng. All authors reviewed the results and approved the final version of the manuscript.

Availability of Data and Materials: All data generated or analysed during this study are included in this published article.

Conflicts of Interest: The authors declare that they have no conflicts of interest to report regarding the present study.

References

1. Development and Reform Commission (2021). Guiding opinions of the national development and reform commission and the energy administration on accelerating the development of new energy storage. *Bulletin of the State Council of the People's Republic of China,* pp. 43–46.

2. Li, J. H., Zhang, J. H., Mu, G., Ge, Y. F., Yan, G. G. et al. (2019). Hierarchical optimal scheduling for deep peak shaving of energy storage-assisted thermal power units. *Power Grid Technology, 43(11),* 3961–3970.

3. Li, J. H., Jiao, J., Yan, G. G., Mu, G., Gao, C. L. et al. (2013). Simulation study on the third-order dynamic model of lead-acid battery. *Journal of Northeast Electric Power University, 33(1),* 103–108.

4. He, H. J., Zhang, N., Du, E. S., Ge, Y., Kang, C. Q. (2020). A review of the operation efficiency and life decay modeling methods of large-scale electrochemical energy storage on the grid side. *Automation of Electric Power Systems, 44(12),* 193–207.

5. Feng, J. Q., Si, Y. W., Wu, L., Huang, K. F., Zhang, X. (2020). Characteristic analysis of power battery based on dynamic comprehensive equivalent circuit model. *Energy Storage Science and Technology, 9(3),* 986–992.

6. Li, J. H., Hu, D. C., Mu, G., Wang, S., Zhang, Z. S. et al. (2020). Optimal control strategy for large-scale VRB energy storage auxiliary power system in peak shaving. *International Journal of Electrical Power & Energy Systems, 120,* 106007.

7. Liu, Y. (2021). *Power distribution strategy of electrochemical energy storage power station participating in secondary frequency regulation of power system (Master Thesis)*. Northeast Electric Power University, China.

8. Liu, D. B., Yuan, Y., Li, S. C., Cao, H. J., Jin, Z. T. et al. (2022). A review of capacity allocation in systems with renewable energy using hydrogen energy storage. *Electrical Measurement and Instrumentation, 59(12),* 1–13.

9. Qin, M. Z., Zhang, G. Y., Qi, D. L. (2016). Modeling and simulation of wind power-hydrogen energy coupling system. *Electronic Technology, 45(8),* 18–23.

10. Ren, Z. Y., Luo, X., Qin, H. L., Jiang, Y. P., Yang, Z. X. et al. (2022). Mid- and long-term optimal operation of a hydrogen-containing regional integrated energy system considering the physical properties of hydrogen storage. *Power Grid Technology, 46(9),* 3324–3333.

11. Gu, T., Yuan, Y. (2021). Simulation modeling and analysis of proton exchange membrane fuel cells. *Power Technology, 45(4),* 459–462.

12. Farrukh, K., Ibrahim, D., Marc, A. R. (2016). Analysis and assessment of an integrated hydrogen energy system. *International Journal of Hydrogen Energy, 41(19),* 7960–7967.

13. Cai, L. D., Li, Q., Liu, Q., Wang, T. H., Yang, W. et al. (2022). An optimal control method for multi-stack fuel cells considering system hydrogen consumption and durability. *Chinese Journal of Electrical Engineering, 42(10),* 3670–3680.

14. Cai, G. W., Kong, L. G. (2016). PEMFC grid-connected power generation system modeling and optimal control. *China Electric Power, 49(11),* 75–81.

15. Cai, G. W., Bian, Y. D., Kong, L. G., Song, J., Xu, H. (2020). Homogeneous modeling of wind/light hydrogen production system. *China Electric Power, 53(10),* 59–65.

16. Amir, R. R., Seyed, M. A., Mohammad, H. N., Ehsanolah, A., Mahdi, S. (2022). A green hydrogen energy storage concept based on parabolic trough collector and proton exchange membrane lectrolyzer/fuel cell: Thermodynamic and exergoeconomic analyses with multi-objective optimization. *International Journal of Hydrogen Energy, 47(62),* 26468–26489.

17. Seyed, M. A., Amir, R. R., Ahmad, A. (2021). Comprehensive assessment and multi-objective optimization of a green concept based on a combination of hydrogen and compressed air energy storage (CAES) systems. *Renewable and Sustainable Energy Reviews, 142,* 1364–0321.

18. Rama, C. M., Paresh, K. (2022). Silicon nanostructures for solid-state hydrogen storage: A review. *International Journal of Hydrogen Energy, 48(4),* 1401–1439.

19. Zhao, X. Y., Chen, H., Zheng, Q. W., Liu, J., Pan, P. Y. et al. (2022). Thermo-economic analysis of a novel hydrogen production system using medical waste and biogas with zero carbon emission. *Energy, 265,* 126333.

20. Mohamed, N., Hamdy, H. (2022). Assessment of hydrogen production from waste heat using hybrid systems of Rankine cycle with proton exchange membrane/solid oxide electrolyzer. *International Journal of Hydrogen Energy, 48(20),* 0360–3199.

21. Liang, Y. F., Liang, Q. C., Zhao, J. F., He, J. N. (2022). Downgrade power allocation for multi-fuel cell system (MFCS) based on minimum hydrogen consumption. *Energy Reports, 8,* 15574–15583.

22. Liu, Y. L., Zheng, J. Y., Xu, P., Zhao, Y. Z., Chen, H. G. (2008). Numerical simulation of the effect of ambient temperature on leakage and diffusion of high-pressure hydrogen storage tanks. *Journal of Engineering Thermophysics, 5,* 770–772.

23. Li, P. G., Qiu, D. K., Shen, S. Y., Peng, L. F. (2021). Research on performance degradation of integrated regenerative fuel cell. *Power Technology, 45(6),* 749–752+796.

24. Zhu, D., Chabane, D., Ait-Amirat, Y., N'Diaye, A., Djerdir, A. (2017). Estimation of the state of charge of a hydride hydrogen tank for vehicle applications. *2017 IEEE Vehicle Power and Propulsion Conference (VPPC)*, pp. 1–6. New York, USA.

25. Xu, Z., Li, X. C., Jia, L. Z., Chen, B., Dai, Z. Q. et al. (2022). The influence of overcharge cycle on the capacity attenuation and safety of lithium-ion batteries. *Energy Storage Science and Technology, 11(12),* 3978–3986.

26. Zhao, J. N., Jin, Y., Wang, S. J., Guo, X. J. (2017). Temperature characteristics and capacity decay model of commercial $Li_4Ti_5O_{12}$ batteries. *Chinese Journal of Electrical Engineering, 37(17),* 5069–5075+5226.

27. Yuan, T. J., Cao, J. L. (2022). Capacity optimization of wind-hydrogen low-carbon energy system considering wind power-load uncertainty. *High Voltage Technology, 48(6),* 2037–2044.

28. Cai, Q. Q., Xiao, Y., Zhu, Y. Q. (2021). A day-ahead economic coordination dispatching model of electric heating microgrid considering electricity-to-hydrogen and fuel cells. *Electric Power Automation Equipment, 41(10),* 107–112+161.

29. Li, Z., Zhang, R., Sun, H. X., Zhang, W. D., Mei, C. X. (2022). A review of key technologies for renewable energy multi-energy complementary production-storage-hydrogen transport. *Journal of Electrotechnical Technology, 36(3),* 446–462.

30. Yan, G. G., Liu, Y., Duan, S. M., Li, H. B., Mu, G. et al. (2020). Power distribution strategy of battery energy storage unit group participating in secondary frequency regulation of power system. *Automation of Electric Power Systems, 44(14),* 26–34.

31. Zhang, C. Z. (2009). *Modeling and simulation research of solar water electrolysis hydrogen production system (Master Thesis).* Southwest Jiaotong University, China.

32. L, Q. (2011). *Research on the modeling and control method of proton exchange membrane fuel cell system (Ph.D. Thesis).* Southwest Jiaotong University, China.

33. Cai, G. W., Chen, C., Kong, L. G., Peng, L., Li, Z. X. (2018). Control strategy of wind hydrogen coupling combined network system. *Journal of Solar Energy, 39(10),* 2970–2980.

34. Wu, J., Yin, Z., Li, H., Zhao, B., Ji, Q. et al. (2021). High-frequency equivalent circuit model of lithium-ion battery based on fractional order theory. *Journal of Electrotechnical Technology, 36(18),* 3902–3910.

35. Mi, L. X. (2021). *Study on the electrolysis characteristics of wind power electrolysis water hydrogen production system (Master Thesis).* Xinjiang Agricultural University, China.

36. Yang, X. B., Zheng, Y. J., Gao, W. K., Ren, D. S., Han, X. B. et al. (2021). Power state estimation of high specific energy energy storage lithium battery system based on improved equivalent circuit model. *Power Grid Technology, 45(1),* 57–66.

37. Liu, X. R., Jiang, Y., Zhang, X. X., Chen, W. R. (2021). A review of three-dimensional numerical simulation of proton exchange membrane fuel cells. *Chinese Journal of Electrical Engineering, 41(21),* 7352–7370.

38. Kong, L. G., Cai, G. W., Chen, C., Xing, L. (2017). Modeling and grid connection control of active permanent magnet direct drive wind turbine based on hydrogen energy storage. *Journal of Electrotechnical Engineering, 32(18),* 276–285.

Appendix A

Appendix A: Electrolyzer and fuel cell model parameters table

Parameter name	Parameter expression	Numerical value	Unit
The number of electrons transferred	z	2	–
Faraday constant	F	96.487	kJ/(V·mol)
Gibbs	ΔG	236.48	kJ/mol
Water activity	aH_2O	1	–
Electrolyzer module area	A_{cell}	0.25	m^2
Electrolyzer temperature	T_{el}	25	°C
Number of serial modules of electrolyzers	N_{el}	80	–
Ohm parameter	r_1	0.000 073	Ωm^2
Ohm parameter	r_2	−0.000 000111	$\Omega m^2 °C^{-1}$

(Continued)

Table A1 (continued)

Parameter name	Parameter expression	Numerical value	Unit
Electrode overvoltage parameters	s_1	0.16	V
Electrode overvoltage parameters	s_2	0.001 38	V/°C
Electrode overvoltage parameters	s_3	−0.000 016	V/°C²
Electrode overvoltage parameters	t_1	0.016	m^2A^{-1}
Electrode overvoltage parameters	t_2	−1.3	$m^2A^{-1}°C$
Electrode overvoltage parameters	t_3	421	$m^2A^{-1}°C^{-2}$
Faraday efficiency coefficient	a_1	99.5	%
Faraday efficiency coefficient	a_2	−9.578 8	m^2/A
Faraday efficiency coefficient	a_3	−0.055 5	$m^2°C/A$
Faraday efficiency coefficient	a_4	1 502.71	m^4/A
Faraday efficiency coefficient	a_5	−70.8	$m^4°C/A$
H2 high calorific value	HHV_{H2}	286	kJ/mol
Entropy change	ΔS	0.164	kJ/(K·mol)
Reference temperature	T_{ref}	298.15	K
Gas constant	R	$8.314\,41 * 10^{-3}$	kJ/(K·mol)
Empirical parameters	ξ_1	0.951 4	V
Empirical parameters	ξ_2	−0.003 12	V/K
Empirical parameters	ξ_3	$-7.4 * 10^{-5}$	V·cm³/(K·mol)
Empirical parameters	ξ_4	$1.87 * 10^{-4}$	V/A/K
Water content	λ	10	–
Film resistivity	r_M	–	Ω·cm
Battery operating factor	B	0.016	–
Maximum battery current density	J_{max}	1.5	A/cm²
PEMFC thickness	l	$51 * 10^{-4}$	cm
Membrane effective area	A	250	cm²
Impeding protons through the membrane impedance	R_c	0.000 3	Ω
PCS efficiency piecewise linearization coefficient	a (inversion process)	0.01797 (P/PN = 0.4∼1) 0.07134 (P/PN = 0.2∼0.4) 0.299 (P/PN = 0.1∼0.2)	–
PCS efficiency piecewise linearization coefficient	a (rectification process)	0.01592 (P/PN = 0.4∼1) 0.06107 (P/PN = 0.2∼0.4) 0.2797 (P/PN = 0.1∼0.2)	–

(Continued)

Table A1 (continued)

Parameter name	Parameter expression	Numerical value	Unit
PCS efficiency piecewise linearization coefficient	b (inversion process)	0.9533 (P/PN = 0.4~1) 0.0.9316 (P/PN = 0.2~0.4) 0.0.8855 (P/PN = 0.1~0.2)	–
PCS efficiency piecewise linearization coefficient	b (rectification process)	0.96 (P/PN = 0.4~1) 0.9418 (P/PN = 0.2~0.4) 0.8976 (P/PN = 0.1~0.2)	–